

LATERAL-ANGULAR AND TEMPORAL CHARACTERISTICS OF EAS OPTICAL RADIATION

Chuykova T.A., Galkin V.I., Ivanenko I.P., Roganova T.M.
Institute of Nuclear Physics, Moscow State University,
Moscow 119899, USSR

The paper presents characteristics of the direct and scattered components of electron-photon shower optical radiation for distances $R \geq 500$ m from the shower core to a detector, allowing for the Cerenkov and fluorescent mechanism of photon generation. The results of calculations can be employed to clarify the techniques for determination of the shower parameters detected by both installations registering fluorescent light and those recording Cerenkov light.

1. Introduction. Optical radiation has been used for many years to investigate the lateral EAS development/1,2/. Each new more accurate and/or detailed consideration of the optical component leads, as a rule, to decreasing uncertainties in the determination of shower parameters and sometimes allows finding new characteristics of the shower optical image, which are more sensitive to the nuclear interaction parameters at superhigh energy or to the shape of the primary cosmic ray spectrum than those used earlier/3/.

One of these improved considerations has been reported in /4,5/ where "contamination" of the fluorescent component of EAS optical radiation by scattered Cerenkov light has been examined, and both lateral-angular and temporal characteristics of the shower optical image has been presented. The author of /4,5/ divides the Cerenkov light registered by a detector into three components: direct (non-scattered) light, scattered light, and fluorescent light, thus assuming that fluorescent photons, unlike to Cerenkov ones, would not scatter in the atmosphere (i.e. the fluorescent light being always only direct). When considering the scattered component, the author confines himself to a single scattering; as a model of longitudinal development of EAS with $E_0 = 10^{17} - 10^{18}$ eV the author have used a cascade curve of a shower induced deep in the atmosphere by a gamma-ray of $E_0 = 2 \cdot 10^{11}$ eV, with the hope that this simplification would not considerably distort the relative contributions of various optical radiation components. The papers /4,5/ furthermore have not presented the temporal characteristics of a direct Cerenkov component. Since the results obtained using the above noted approximations, on one hand, are only preliminary and, on the other hand, seem to be important and interesting, we attempted to consider this group of phenomena with the help of simulating program of a different type.

2. The present paper approach. A separate consideration of the Cerenkov and fluorescent components undoubtedly gives an additional information of their relative contributions, however most of modern installations are incapable of dis-

tinguishing the nature of photons arriving at a detector.

We performed calculations for a 3000-8000Å wavelength-band. Since large distances ($R \geq 500\text{m}$) from the core to a detector are considered at which the characteristic temporal scale of a pulse is $\sim 100\text{ ns}$, the time of fluorescent photon reemission can be neglected in the first approximation. Thus, in the situation of interest for us the differences between the two components reduce to their angular characteristics which practically do not affect the simulation algorithmic aspect. So, a unified source of photons is used composed of Cerenkov and fluorescent sources with appropriate angular characteristics and intensities, and the photon transfer from this source to a detector is considered as usually introducing the photon time delay:

$$CT = r - r_0 + H_0 \gamma_0 \left(\frac{\exp(z/H_0) - 1}{\cos \theta} - \frac{\exp(z_0/H_0) - 1}{\cos \theta_0} \right), \text{ where } H_0 = 7.5\text{km} \quad (1)$$

is the exponential atmosphere depth; $\gamma_0 = 2.9 \cdot 10^{-4}$ is the diversity from a unity of an atmosphere refraction index at sea level; $\vec{r}_0 = (r_0, \theta_0, \psi_0)$ being the shower generation point; $\vec{z}_0 = r_0 \cos \theta_0$; $\vec{r} = (r, \theta, \psi)$ is the point under consideration; $z = r \cos \theta$; the spherical coordinate system is bound to a detector.

As far as a large core distances region is concerned a simple shower model—that of a moving point—is valid, i.e. we neglect the electron lateral distribution and take into account their angular distributions only. The direct optical radiation component is calculated on average. Use is made of a model of the angular distribution /6/, $f(\theta)$ where α is calculated using moments $\overline{\theta^2}$ also present in /6/. The cascade curve approximation used is $N(\epsilon_0, \epsilon, s) = \frac{\epsilon_0 s}{(1 + \epsilon) s} \cdot \frac{1}{q(s)}$ (2)

where $\epsilon = ED(s)/\beta$, $\epsilon_0 = E_0 D(s)/\beta$, $\beta = 81\text{ MeV}$, $D(s)$ and $q(s)$ are the known cascade functions from /7/.

For the Cerenkov component E is the threshold energy of Cerenkov light, and for the fluorescent component $E = 0$. A charged particle is assumed to produce 5 photons over a meter of path due to the fluorescent mechanism. The scattered component was Monte-Carlo simulated. Over each segment of the shower trajectory, approximately 0.1 c.u. long, 6×13 photons (6 cells over the azimuth and 13 cells over the polar angle) were radiated and followed till their arrival at a detector, till their absorption by the Earth's surface, till their leaving the atmosphere or till their departure from a detector to a distance larger than some value. When arriving at a detector, a photon was given a weight factor proportional to the overall light amount radiated by the shower electrons over a fixed trajectory segment and to the weight of angular cell from which centre of mass the photon has been radiated. The differential cross section of scattered light was, as in /4,5/, proportional to $(1 + \cos^2 \chi)$, where χ is the scattering polar angle. The data on the scattering length (molecular Rayleigh and aerosol) were taken from /8/. The detector comprised 200 temporal bins each of 10 ns and one integral bin for delays $> 2000\text{ ns}$. The angle 2π ster was divided into 120 bins (12 equal-size bins over the azimuth angle $\times 10$ equal-size bins over the polar angle) covering

different solid angles (.04 ster to .08 ster). Though the program can simulate inclined showers, the present paper reports on the results for the vertical electron-photon showers with $E_0=10^{17}$ eV for distances $R=.5, 2.0, 8.0$ km from detector. For a better comparison with the results of /4,5/ we considered production depth 119 g/cm^2 ($H=16.1$ km) that yields $t_m=896 \text{ g/cm}^2$ and the same distance $H_{\text{obs}}-H_m=1.2$ km, as in /4,5/. For each R the data on scattered light were obtained by averaging over 10 showers.

3. Simulation results. The lateral-angular distribution of the light in Fig.1 (the solid curves are for the present calculation, the dash-dot ones - /4,5/- the sum of direct Cerenkov and fluorescent photons, the dashed curves are for scattered Cerenkov light /4,5/). All the data are divided by detector solid angles; The data /4,5/ are furthermore multiplied by $5 \cdot 10^7$ to allow for the differences in primary energies. The present paper data were selected from the bins facing the shower core. Unlike to the data /4,5/, our curves for scattered light do not reveal such an abrupt rise with zenith angle, though an increase of scattered light in the overall flux is noticeable even at $R=.5$ km that is explained by a decreasing contribution of the Cerenkov mechanism. At $R=8$ km, the two sets of data are the most similar, though some differences in intensity are observed which can be explained by the diversity between the cascade curves and solid angles of detectors in /4,5/ and present paper.

Fig.2 shows the data on FWHM τ of scattered light pulses. FWHM of the scattered component, according to our calculation, is noticeably broader than that of the direct one (multiple scattering really matters) and increases with R , though slower than FWHM of the direct component. In the present paper FWHM increases with zenith angle similar to that in /4/. Fig.3 shows typical pulses for the direct and scattered components (integrated over all bins facing the shower core).

References

1. Jelly J. Cerenkov radiation, Moscow, 1960.
2. Nesterova N.M., Chudakov A.E., 1962, JETP, 42, vyp6, 1622.
3. Galkin V.I., Makarov V.V., 1983, 18th ICRC, v.6, 236.
4. Protheroe R.J., 1982, J. Phys. G., v.8, L165.
5. Protheroe R.J., 1983, Proc. 18th ICRC, v.6, 240.
6. Belyaev A.A. et al. Electron-photon showers in cosmic rays at superhigh energies, 1980, Moscow.
7. Belenky S.Z. Avalanche processes in cosmic rays, 1984, Moscow.
8. Martynov A.Ya. Course of applied astrophysics, 1964, Moscow.

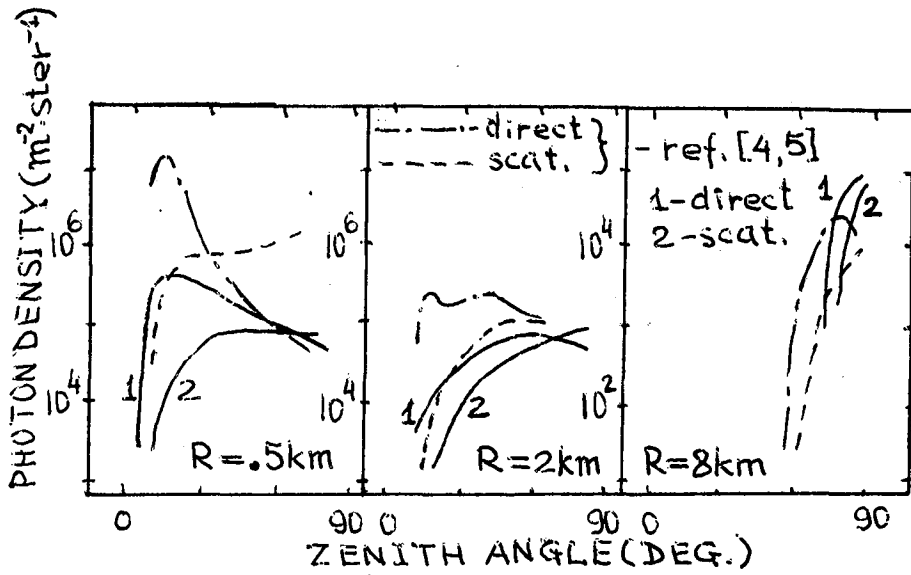


FIG. 1

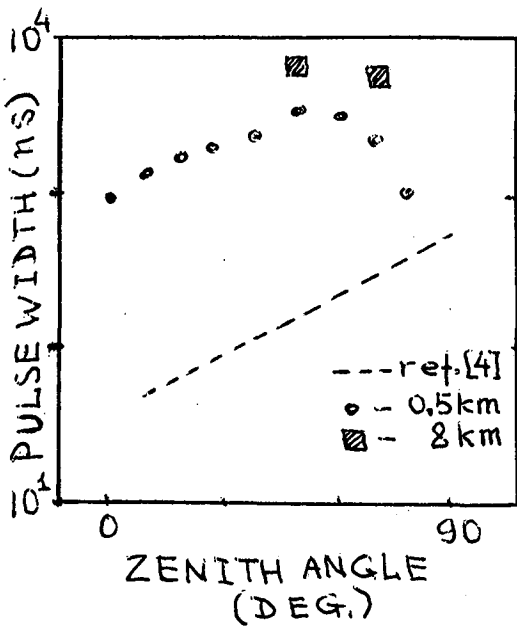


FIG. 2

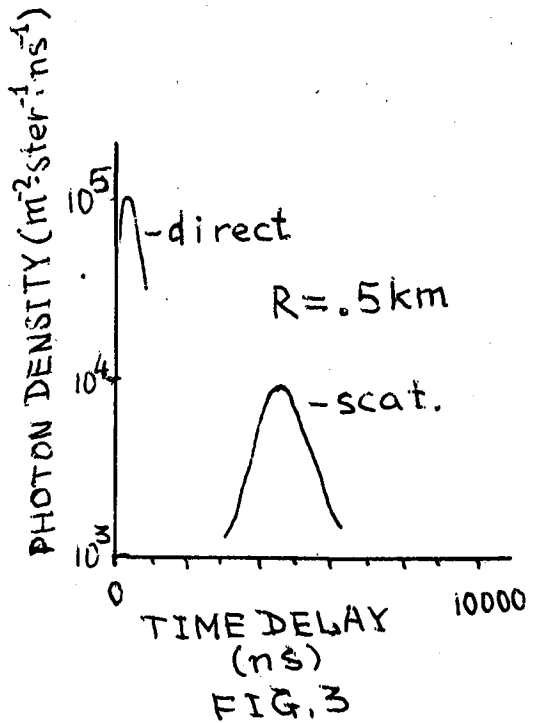


FIG. 3